Hindawi
Journal of Nanomaterials
Volume 2019, Article ID 8252036, 12 pages
https://doi.org/10.1155/2019/8252036

Research Article

Multiresponsive Poly(*N*-Acryloyl glycine)-Based Nanocomposite and Its Drug Release Characteristics

Nunthiya Deepuppha, Sudarat Khadsai, Boonjira Rutnakornpituk, Uthai Wichai, and Metha Rutnakornpituk

Department of Chemistry and Center of Excellence in Biomaterials, Faculty of Science, Naresuan University, Phitsanulok 65000, Thailand

Correspondence should be addressed to Metha Rutnakornpituk; methar@nu.ac.th

Received 22 May 2018; Accepted 29 October 2018; Published 27 January 2019

Academic Editor: Domenico Acierno

pH- and thermoresponsive nanocomposite composed of poly(*N*-acryloyl glycine) (PNAG) matrix and magnetite nanoparticle (MNP) was synthesized and then used for drug controlled release application. The effects of crosslinkers, e.g., ethylenediamine and *tris*(2-aminoethyl)amine, and their concentrations (1 and 10 mol%) on the size, magnetic separation ability, and water dispersibility of the nanocomposite were investigated. The nanocomposite crosslinked with *tris*(2-aminoethyl)amine (size ranging between 50 and 150 nm in diameter) can be rapidly separated by a magnet while maintaining its good dispersibility in water. It can respond to the pH and temperature change as indicated by the changes in its zeta potential and hydrodynamic size. From the in vitro release study, theophylline as a model drug was rapidly released when the pH changed from neutral to acidic/basic conditions or when increasing the temperature from 10°C to 37°C. This novel nanocomposite showed a potential application as a magnetically guidable vehicle for drug controlled release with pH- and thermotriggered mechanism.

1. Introduction

Magnetite nanoparticle (MNP) has attracted great attention in recent years in biomedical and biotechnological applications [1–5] owing to its magnetically guidable properties [2], high surface area-to-volume ratio [4], high saturation magnetization [6, 7], low toxicity, and high biocompatibility [8]. These intriguing properties make MNP as an ideal candidate for use in various biomedical fields such as drug delivery [5], diagnostics, therapeutics [2, 9, 10], and magnetic separation [11–13].

In the magnetic separation application, MNP should have high magnetic responsiveness, so that it should abruptly respond to a magnet and completely remove unadsorbed entities after decanting [14, 15]. Formation of nanocomposite containing multiparticles of MNP embedded in polymer matrix was another promising approach to enhance magnetic sensitivity while maintaining its good dispersibility in the media. When individual unique properties of both MNP and polymer matrix were combined, multifunctional nanocomposite serving as a platform for further conjugation with desirable bioentities can be obtained [16, 17]. Thus, this hybrid nanocomposite has been particularly used in the biological field such as drug delivery system [18, 19], controlled release [16, 20, 21], and magnetic separation [11–13]. Previous works have reported the synthesis of MNP-polymer nanocomposite having both good magnetic separation ability and good water dispersibility for drug controlled release [4, 16] and for conjugation with bioentities [17, 22].

Interestingly, polymer matrix having external stimuli-responsive properties in nanocomposite can be used as a handle in controlled release applications [23–27]. Previous works have presented the use of MNP coated with pH- and thermoresponsive polymers as a handle for triggered mechanisms for drug controlled release [26]. Among the pH- and thermo-responsive polymers, poly(*N*-acryloyl glycine) (PNAG) is of particular interest in this research because it can be facilely synthesized via a free radical polymerization

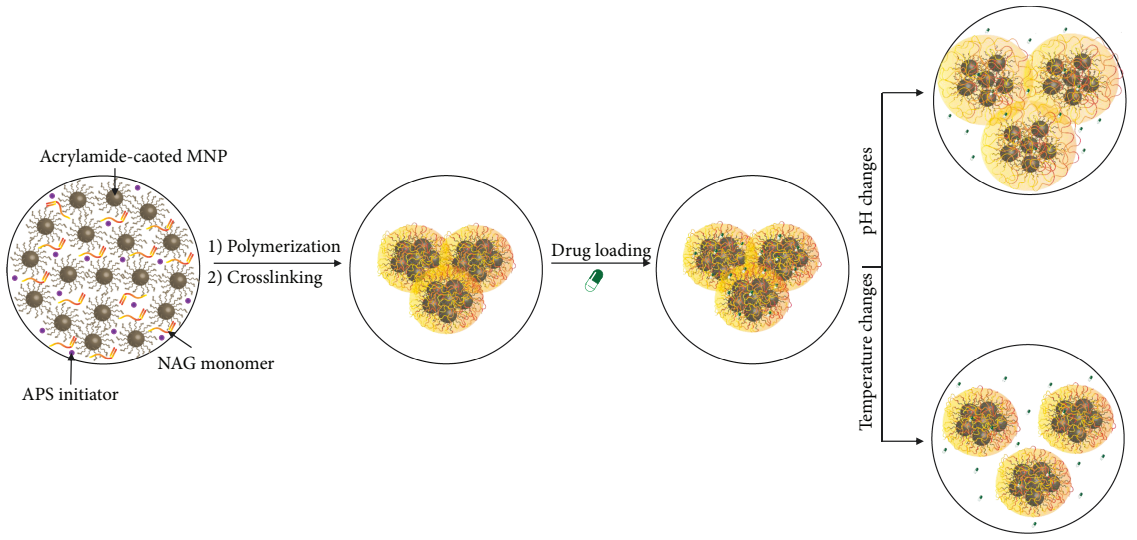

Figure 1: Schematic preparation of PNAG-coated MNP nanocomposite for drug controlled release applications.

of *N*-acryloyl glycine monomer in aqueous solutions [12, 28]. H-bonding network of carboxyl groups (-COOH) and amide groups (-CONH-) in PNAG chains with water molecules plays a crucial role in its pH- and temperature-responsive properties [29].

In a basic pH condition, the carboxylate groups (COO^-) of PNAG should be formed, resulting in the enhancement in water swelling due to negative-charge repulsion among the chains. On the other hand, when the polymer was protonated in an acidic pH condition, its collapsed structure should be formed [30]. PNAG also showed thermoresponsive properties when its environmental temperature changed due to H-bonding of amide bonds in the chains with water molecules [31, 32], similarly to the case of the amino acid-derived polymers, such as poly(*N*-acryloyl glycinamide) (PNAGA) [33], poly(acrylamide) (PAAm), and poly(acrylic acid) (PAA) [34–36]. However, the study in upper critical solution temperature (UCST) of PNAG homopolymer has never been reported, while that of PNAG-containing copolymer was very limited [37]. At the temperature below the UCST, PNAG should be stabilized by intramolecular H-bonding, resulting in the formation of solid hydrogels. At the temperature above its UCST, it can reversibly turn into fluid state because the intramolecular H-bonding is diminished and because of the simultaneous formation of intermolecular H-bonding between water molecules and chains of polymer [33].

This work reports the synthesis of MNP nanocomposite coated with pH-/thermoresponsive PNAG and its use in drug controlled release. Modification of MNP surface with PNAG was first prepared via a free radical polymerization, followed by a crosslinking reaction. Different types and concentrations of the crosslinkers (1 mol% and 10 mol% of *tris*(2-aminoethyl)amine or ethylenediamine) were used in the crosslinking in an attempt to tune the reaction condition to gain the nanocomposite with good water dispersibility and high magnetic separation ability. The effect of the crosslinking condition of the nanocomposite on the controlled release of theophylline as a model drug was also investigated. It was rationalized that PNAG can serve as a reservoir of the drug with both pH- and temperature-triggered drug release mechanisms (Figure 1). The effects of pH (pH 2.0, pH 7.4, and pH 11.0) and temperature (10°C and 37°C) on its drug release rate were also herein investigated.

2. Experimental

2.1. Materials. Ammonium hydroxide (NH_4OH) (28–30%, J.T. Baker), *N*-(3-dimethylaminopropyl)-*N*′-ethylcarbodiimide hydrochloride (EDC·HCl) (GL Biochem Shanghai Ltd.), ethylenediamine (Carlo Erba), glycine (AR grade), iron(II) chloride tetrahydrate ($FeCl_2.4H_2O$) (99%, Acros Organic), iron(III) chloride ($FeCl_3$) (98%, Acros), oleic acid (Carlo Erba), ammonium persulfate (APS) (98%, Carlo Erba), (3-aminopropyl) triethoxysilane (APTES) (99%, Acros), triethylamine (TEA) (97%, Carlo Erba), theophylline anhydrous (≥99%, Sigma-Aldrich), and *tris*(2-aminoethyl)amine (96%, Sigma-Aldrich) were used as received. Acryloyl chloride was prepared via a chloride exchange reaction between benzoyl chloride (Acros, 99%) and acrylic acid (98%, Acros) at 75°C to obtain a colorless liquid with 60% yield.

2.2. Characterization. Fourier-transform infrared spectrometry (FTIR) was conducted on a Perkin–Elmer Model 1600 series FTIR spectrometer. ^{1}H NMR spectroscopy was characterized via a 400 MHz Bruker NMR spectrometer. Transmission electron microscopy (TEM) was conducted on Philips Tecnai 12 operated at 120 kV. The dispersion of the particle in water was dropped on a carbon-coated copper grid at room temperature without filtration. Zeta potential and hydrodynamic size (D_h) of the particle were determined on NanoZS4700 nanoseries Malvern photocorrelation spectrometer (PCS). Magnetic properties were characterized via a Standard 7403 Series, Lakeshore vibrating sample magnetometer (VSM). UV-visible spectrophotometry was conducted on Analytik-Jena AG Specord 200 plus UV-Vis spectrophotometer at $\lambda = 272$ nm.

2.3. Preparation of N-Acryloyl Glycine (NAG) Monomer. Glycine (61.8 mmol, 4.64 g) was dissolved in a NaOH aqueous solution (123.6 mmol, 4.95 g). An acryloyl chloride solution in tetrahydrofuran (61.8 mmol, 5.0 mL) was added into the solution and then stirred at 0°C for 3 h. The mixture was washed with diethyl ether, and then the aqueous solution layer was adjusted to a pH 2 solution with conc. HCl. The extraction with ethyl acetate was carried out, and then the organic layer was dried with anh. Na_2SO_4, filtered, and evaporated in vacuo. Finally, white solid as a product was obtained: 2.41 g, 30% yield; ^{1}H NMR (400 MHz, D_2O): δ 4.08 ppm (*s*, 2H), 5.82–5.84 (*dd*, 1H), and 6.24–6.39 (*dd* and *t*, 2H).

2.4. Preparation of Acrylamide-Coated MNP. 30% NH_4OH solution (5.0 mL) was added into a solution mixture of $FeCl_2{\cdot}4H_2O$ (2.1 mmol, 0.83 g) and $FeCl_3$ (2.5 mmol, 0.50 g) with stirring at 25°C for 30 min. After being separated and washed with distilled water, an oleic acid solution (1.0 mL) in toluene (9.0 mL) was added into the MNP dispersion and then stirred at 25°C for 30 min. Oleic acid-coated MNP was precipitated in acetone, separated by a magnet, and then redispersed in toluene (10.0 mL). TEA (13.6 mmol, 1.0 mL) and APTES (11.9 mmol, 2.5 mL) were then added to the dispersion with stirring at 25°C under N_2 for 24 h to obtain amino-coated MNP.

After magnetic separation, washing, and evaporation until dryness, amino-coated MNP (0.05 g) was then dispersed in a NaOH solution (1.50 g) by ultrasonication. An acryloyl chloride (49.5 mmol, 5.0 mL) was slowly added into the MNP dispersion at 0°C in an ice bath for 1 h, and then the mixture was continuously stirred at 25°C for 24 h. After a reaction was completed, the particle was separated by a magnet and then repeatedly washed with distilled water and stored in the dispersion form (0.02 g MNP/mL H_2O).

2.5. Preparation of PNAG-Coated MNP Nanocomposite. NAG monomer (0.25 g, 1.94 mmol) was dissolved in distilled water (20.0 mL), followed by an addition of a dispersion of acrylamide-coated MNP (0.05 g MNP in 25.0 mL distilled water). An APS radical initiator solution (10% in distilled water, 0.04 mmol) was injected into the mixture, and the reaction was set allowed for 2 h at 70°C under N_2 gas to obtain PNAG-coated MNP nanocomposite. After magnetic separation and washing with distilled water to remove the unreacted monomers and uncoated polymer chains, the nanocomposite was then dried in vacuo. In the crosslinking reaction, the dispersion of the nanocomposite (0.05 g nanocomposite in 50.0 mL distilled water) was added with EDC·HCl (5% in distilled water) as a coupling agent and stirred at 25°C 1 h. After magnetic separation, the nanocomposite was redispersed in the crosslinker solutions (1 or 10 mol% of ethylenediamine or *tris*(2-aminoethyl)amine in a pH 11 buffer solution) and then stirred for 1 h. After the crosslinking reaction, the MNP nanocomposite was rinsed with distilled water with the use of a magnet to wash the unreacted crosslinking agents and then dried in vacuo.

2.6. The Release Studies of Entrapped Theophylline from the MNP Nanocomposite. The dispersion of the MNP nanocomposite (5 mg of the MNP nanocomposite in 1.0 mL aqueous dispersion) was dropwise added with a theophylline solution (1.0 mL, 10 mg/mL in distilled water). After stirring for 3 h at 40°C, the drug-loaded MNP nanocomposite was removed from an excess drug using an external magnet. In the *in vitro* release study, the theophylline-entrapped MNP nanocomposite (5 mg of the MNP nanocomposite) was dispersed in 5.0 mL buffer solutions (pH 2.0, pH 7.4, or pH 11.0). The dispersion was placed into a water bath at 10°C or 37°C. At a predetermined time interval, 100 μL of sample dispersion was withdrawn from the release media. After each sampling, the nanocomposite was magnetically separated and then the supernatant was analyzed via UV-visible spectrophotometer at 272 nm wavelength. Percent release (%) was estimated from the following equation;

$$\text{Percent release}\,(\%) = \frac{\text{weight of the release drug at a given time}}{\text{weight of the drug entrapped in the MNP nanocomposite}} \times 100. \quad (1)$$

To determine drug entrapment efficiency (EE) and drug loading efficiency (DLE), the weight of theophylline entrapped in the MNP nanocomposite was determined from the amount of the drug at the maximum point of the release profile combined with those remaining in the particles. The nanocomposite was extracted with a 0.1 M HCl solution to dissolve the leftover drug and then analyzed via UV-visible spectrophotometer. Therefore, EE and DLE were defined from the following equations:

$$\text{EE}\,(\%) = \frac{\text{weight of the drug entrapped in the MNP nanocomposite}}{\text{weight of the loaded drug}} \times 100, \quad (2)$$

$$\text{DLE}\,(\%) = \frac{\text{weight of the drug entrapped in the MNP nanocomposite}}{\text{weight of the MNP nanocomposite}} \times 100. \quad (3)$$

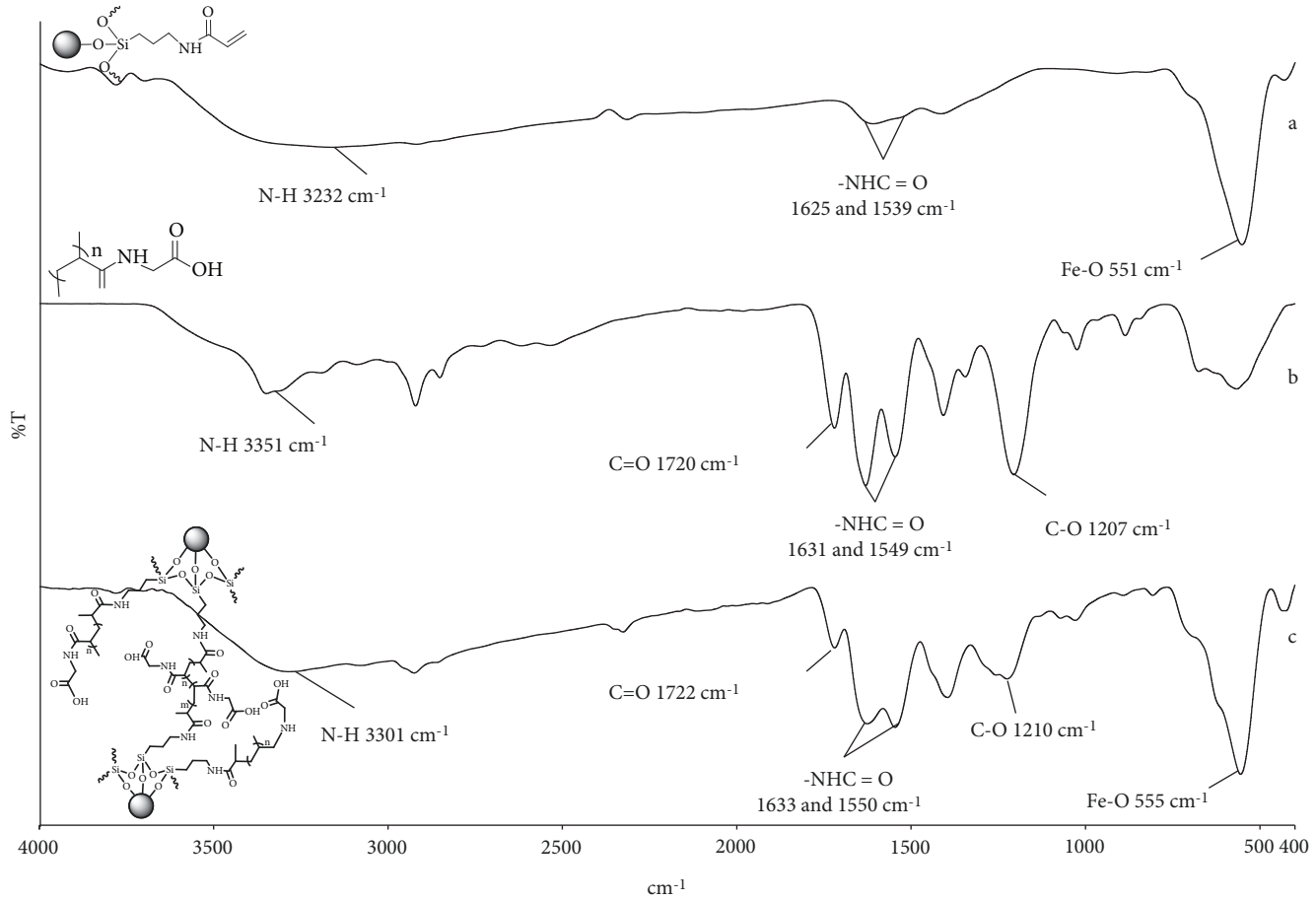

Figure 2: FTIR spectra of (a) acrylamide-coated MNP, (b) PNAG homopolymer, and (c) PNAG-coated MNP nanocomposite.

3. Results and Discussion

In this work, PNAG-coated MNP was first synthesized via a free radical polymerization to form a water dispersible magnetic nanocomposite. In addition to steric stabilization, PNAG also provided electrostatic repulsion stabilization to the nanocomposite due to the presence of carboxylate groups. Additional crosslinking of the MNP nanocomposite was conducted to obtain those with good magnetic separation ability while retaining its good water dispersibility. Two different crosslinkers (ethylenediamine and *tris*(2-aminoethyl)amine) were used in this work to study the effect of the crosslinkers and their concentrations on D_h, water dispersibility and magnetic separation ability of the MNP nanocomposite. pH- and thermoresponsive properties of PNAG coated on its surface provided dual triggering mechanisms for drug release. In this report, in vitro release profile of theophylline entrapped on the nanocomposite was investigated as a function of pH (2.0 7.4 and 11.0) and temperature (10°C and 37°C).

3.1. Characterization of the MNP Nanocomposite. FTIR spectra of the particles before and after coating with PNAG are displayed in Figure 2. The spectrum of acrylamide-coated MNP shows the weak signals of NHC=O stretching (1539 and 1625 cm^{-1}), N-H stretching (3232 cm^{-1}), and also those of the MNP core at 551 cm^{-1} (Fe-O stretching) (Figure 2(a)). Once the nanocomposite was formed by coating MNP with PNAG, the peaks attributed to C-O stretching (1221 cm^{-1}), NHC=O stretching (1550 and 1633 cm^{-1}), C=O stretching (1722 cm^{-1}), and N-H stretching (3301 cm^{-1}) were observed (Figure 2(c)). These signals corresponded well to those of PNAG homopolymer (Figure 2(b)), indicating the presence of PNAG coated on the MNP nanocomposite.

3.2. Effect of Crosslinking Reactions on the Properties of the MNP Nanocomposite. Ethylenediamine and *tris*(2-aminoethyl)amine with two different concentrations (1 and 10 mol%) were used as the crosslinkers in the nanocomposite. The goal of this work was to obtain the MNP nanocomposite with good magnetic separation ability while retaining its good water stability; the conditions in the crosslinking reactions (type of crosslinkers and concentrations) were thus optimized. Zeta potentials and D_h of the nanocomposites were investigated using the PCS technique (Figure 3).

As compared to acrylamide-coated MNP, PNAG-coated MNP nanocomposite did not show an increase in D_h while its zeta potential values significantly increased from −12 to −24 mV, and this was probably due to the existence of anionic carboxylate groups from PNAG. This result well corresponded to that observed from the conductometric

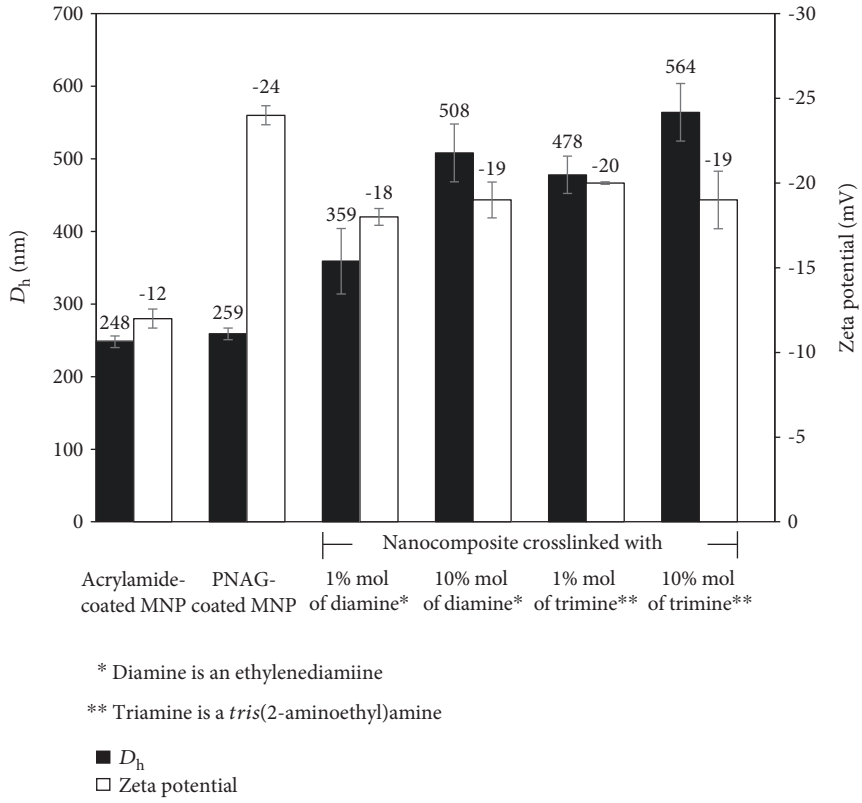

FIGURE 3: D_h and zeta potential values of acrylamide-coated MNP, the MNP nanocomposite (before crosslinking), the MNP nanocomposites after crosslinking with 1 mol% and 10 mol% of ethylenediamine, and 1 mol% and 10 mol% of *tris*(2-aminoethyl)amine.

titration shown in supporting information. After the crosslinking reactions, D_h of all samples significantly increased while its zeta potential values decreased. The coupling reactions between the carboxyl groups of PNAG coated on the particles and the amino groups of the crosslinkers induced the nanoaggregation of the individual particles, resulting in the formation of nanocomposite having multiple particles embedded and a slight drop in the degree of negative charge. The increase in the crosslinker concentration from 1% to 10% also promoted the formation of the crosslinked nanocomposite as indicated by the enlarged D_h. Interestingly, the use of *tris*(2-aminoethyl)amine seemed to enhance the degree of crosslinking as compared to that of ethylenediamine (at the same crosslinker concentrations), probably due to the higher number of the equivalent reactive amines in the reactions (Figure 4).

The size and the size distribution of the MNP nanocomposite in each step of the reactions were also observed via TEM (Figure 5). Acrylamide-coated MNP exhibited aggregation of the particles without the formation of nanoclusters owing to the lack of polymer coating (Figure 5(a)). When MNP surface was coated with PNAG, the particles showed an improvement in water dispersibility without significant aggregation (Figure 5(b)). After the crosslinking, the cluster feature of the nanocomposite with the size of ca. 50–150 nm in diameter was observed (Figures 5(c)–5(f)) and this corresponded to that observed in PCS results. However, there was no apparent difference in the size and the size distribution of the nanocomposite between those crosslinked with ethylenediamine and *tris*(2-aminoethyl)amine or with different concentrations.

Water dispersibility, stability, and magnetic separation ability of the particles in each step of the reactions were investigated. Acrylamide-coated MNP aggregated within a few minutes after the preparation due to a lack of polymeric stabilization. After coating with PNAG, the particles were well stabilized through both steric and electrostatic repulsion mechanisms, resulting in the stable MNP dispersions with insignificant aggregation even after 24 h of the preparation. However, they cannot be completely separated after applying with a magnet for 5 min, which would be troublesome when employed for magnetic separation applications. The crosslinking of these nanocomposites was conducted in an attempt to enhance the magnetic separation ability, while retaining its good water stability. *tris*(2-aminoethyl)amine and ethylenediamine with two different concentrations (1 mol% and 10 mol%) were used as additional crosslinkers. According to the results in Table 1, the nanocomposites after crosslinking showed a fair dispersibility in water after 24 h standing with a slight aggregation. This was probably due to the formation of the nanoclusters with a larger size, which corresponded well to the results observed from the PCS technique discussed above. These nanocomposites can be separated within 5 min due to the increase in its size, resulting

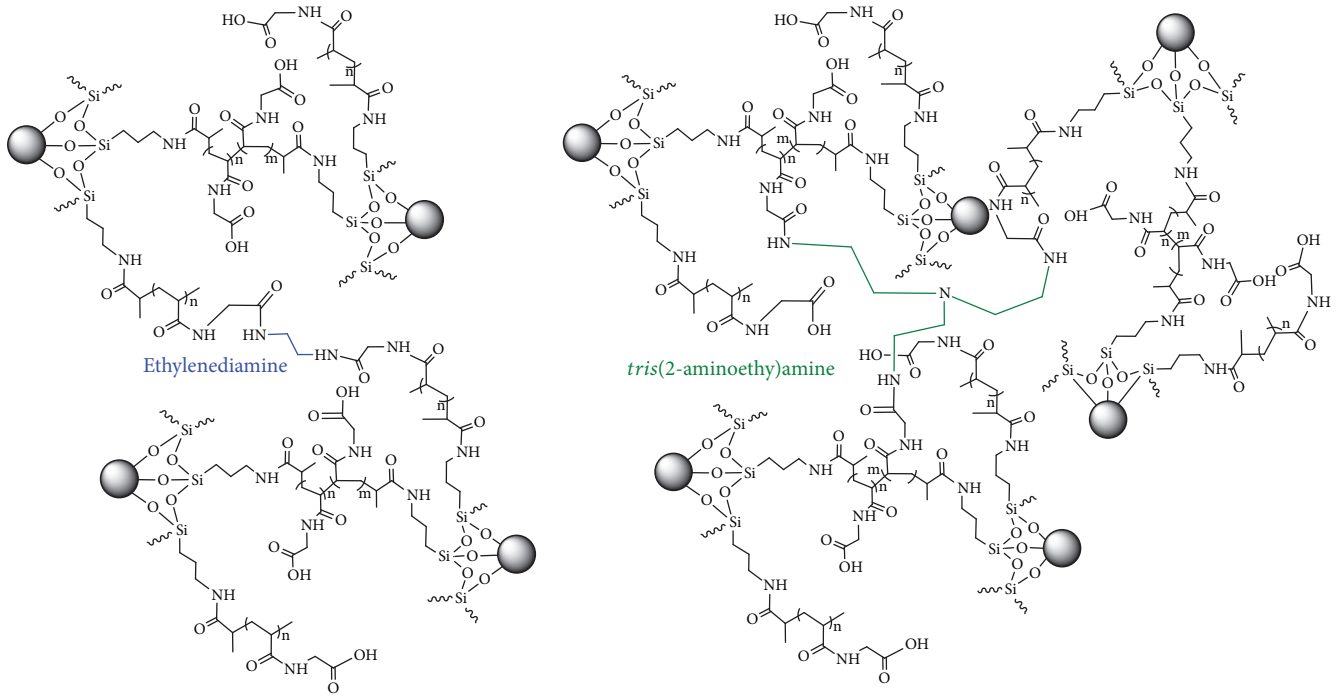

Figure 4: The proposed mechanism of the crosslinking amidations of PNAG-coated MNP with (a) ethylenediamine and (b) *tris*(2-aminoethyl)amine.

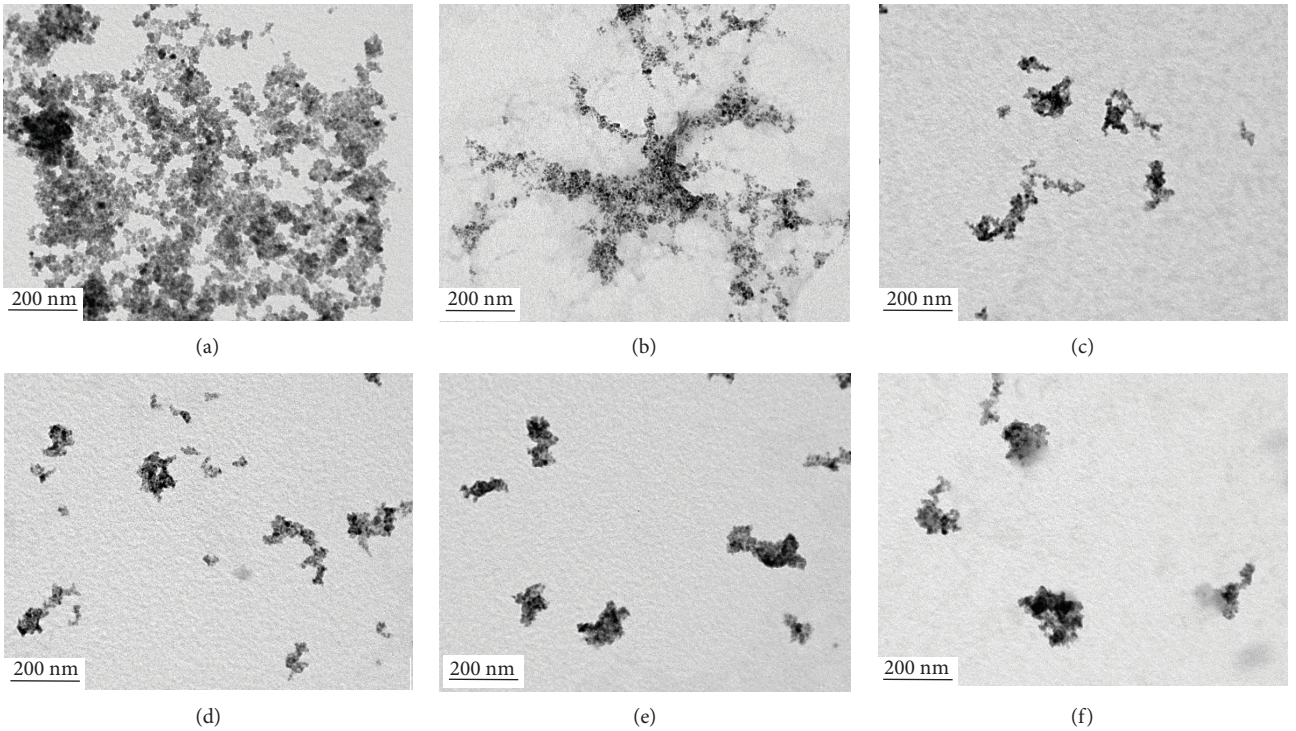

Figure 5: TEM of (a) acrylamide-coated MNP, (b) the MNP nanocomposite (before crosslinking), the MNP nanocomposite after crosslinking with (c) 1 mol% and (d) 10 mol% of ethylenediamine, and (e) 1 mol% and (f) 10 mol% of *tris*(2-aminoethyl)amine.

in an improved response to a magnet. Interestingly, as compared to the others, those crosslinked with 10 mol% *tris*(2-aminoethyl)amine can be completely separated from the dispersion and it would be used as a representative for other studies, e.g., magnetic properties, drug entrapment, and controlled release studies.

Table 1: The effect of crosslinking agents and their concentrations on water dispersibility and magnetic separation ability.

Acrylamide-coated MNP (no PNAG coating)	PNAG coating (before crosslinking)	After crosslinking with			
		1 mol% of diamine*	10 mol% of diamine*	1 mol% of triamine**	10 mol% of triamine**
At initial time					
Dispersibility in water *After 24* h					
Magnetic separation ability *After 5* min					

*Diamine is ethylenediamine. **Triamine is *tris*(2-aminoethyl)amine.

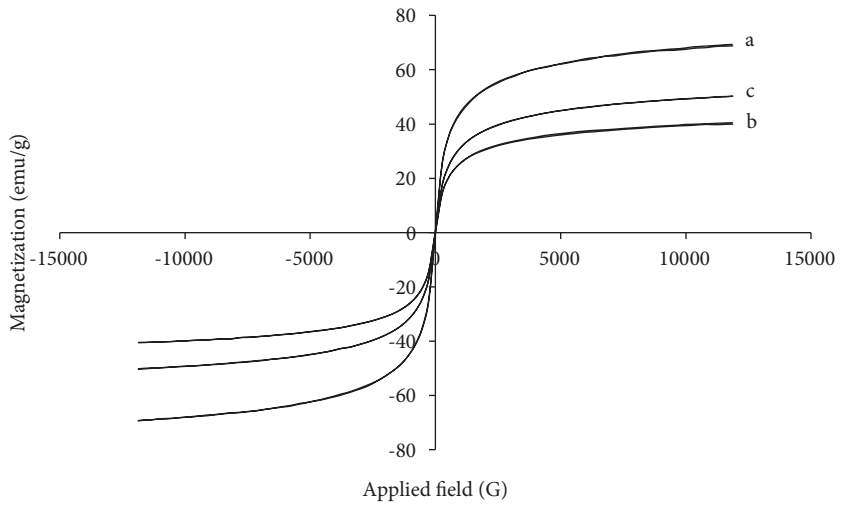

Figure 6: M-H curves of (a) acrylamide-coated MNP, (b) the MNP nanocomposite (before crosslinking), and (c) the MNP nanocomposites after crosslinking with 10 mol% of *tris*(2-aminoethyl)amine.

3.3. Multiresponsive Properties of the MNP Nanocomposite as a Function of Magnetic Field, Dispersion pH, and Temperature. Magnetic properties of acrylamide-coated MNP and PNAG-coated MNP nanocomposites before and after crosslinking with 10 mol% of *tris*(2-aminoethyl)amine were determined via the VSM technique. It was found that the saturation magnetization (M_s) of the particles decreased from 68 emu/g to 40 emu/g after coating with PNAG due to

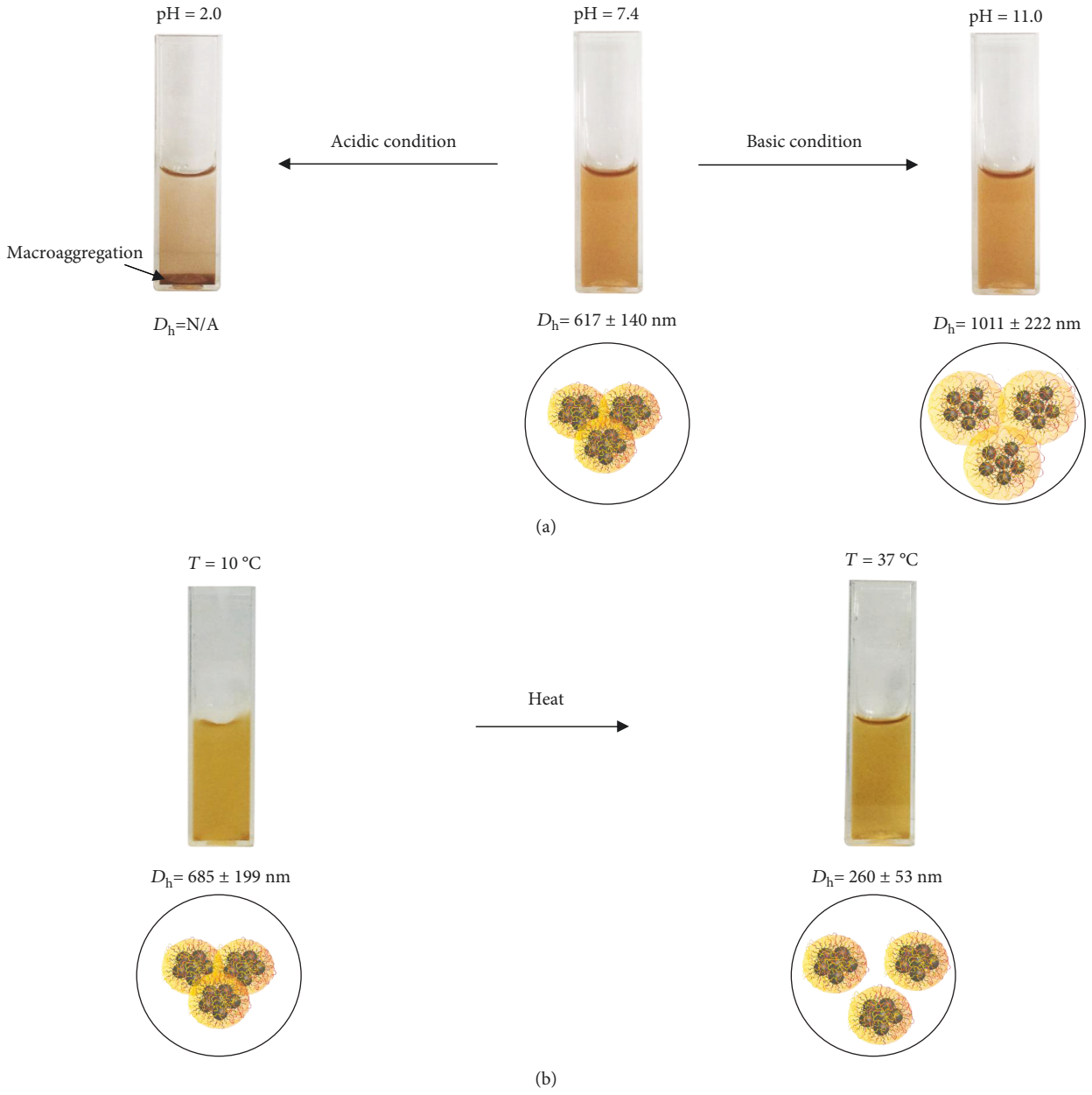

Figure 7: (a) pH- and (b) thermo-responsive properties of the MNP nanocomposite after crosslinking with 10 mol% of *tris*(2-aminoethyl)amine.

the presence of nonmagnetic organic polymer in the nanocomposite (Figure 6). After the crosslinking reaction, its M_s value increased to 50 emu/g and this was probably owing to the formation of MNP nanoclusters, leading to the increase in the magnetic sensitivity [15].

To confirm pH-responsive properties of the crosslinked MNP nanocomposite, its D_h was determined in pH 2.0, 7.4, and 11.0 buffer solutions. It was found that D_h in pH 2.0 cannot be measured due to macroaggregation of the particles (indicated by an arrow in the inset in Figure 7(a)). This was probably because PNAG was in the COOH form, resulting in the lack of anionic charged repulsion. In addition, its D_h increased from 617 nm to 1011 nm when the pH changed from pH 7.4 to pH 11.0 and this was attributed to presence of negatively charged repulsion of -COO^- from PNAG chains, resulting in the swelling of the nanocomposite. The change of D_h as a function of dispersion pH corresponded to the pK_a value of PNAG (pK_a 3.2) in terms of the protonated/deprotonated forms of the carboxyl groups [38]. D_h of the MNP nanocomposite was then investigated at 10°C and 37°C in pH 7.4 buffer solutions. D_h significantly dropped from 685 nm to 260 nm when the temperature was decreased from 10°C to 37°C (Figure 7(b)). It was rationalized that a number of the crosslinked MNP nanocomposites might be in the agglomerated form at 10°C due to the H-bonding among each nanocomposite.

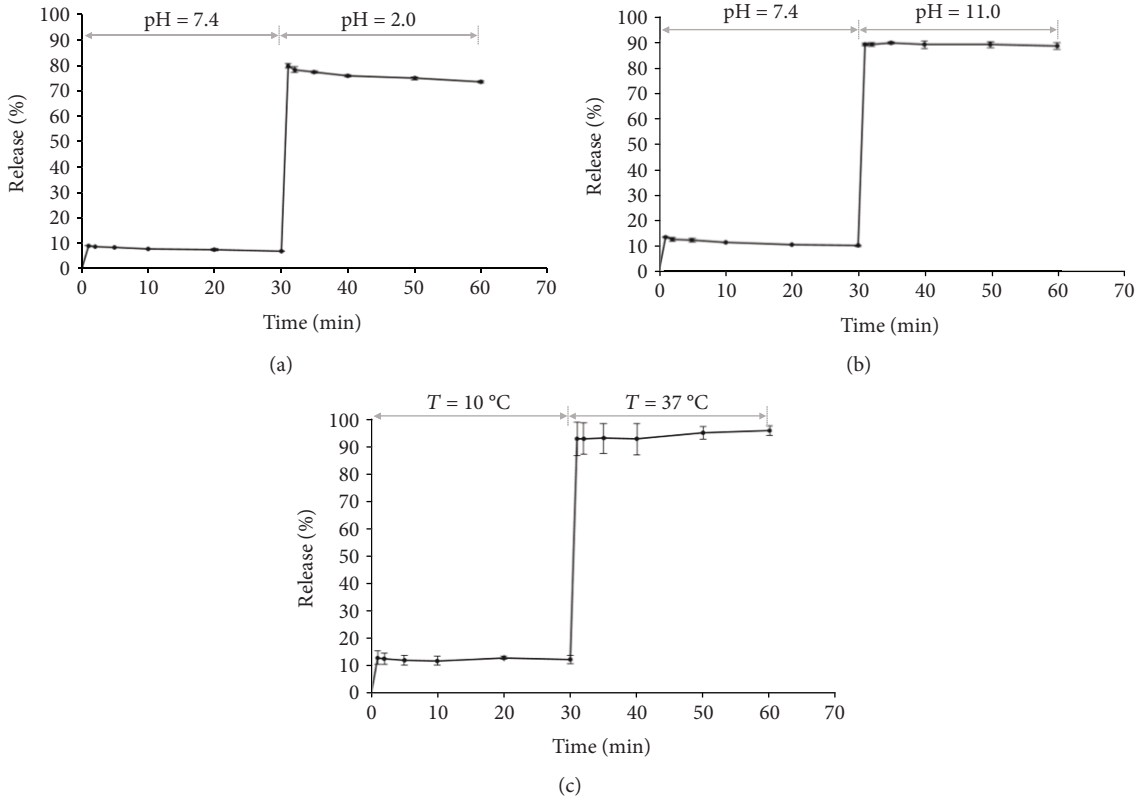

Figure 8: (a, b) The effect of pH and (c) temperature on the theophylline release profiles from the MNP nanocomposite crosslinking with 10 mol% of *tris*(2-aminoethyl)amine.

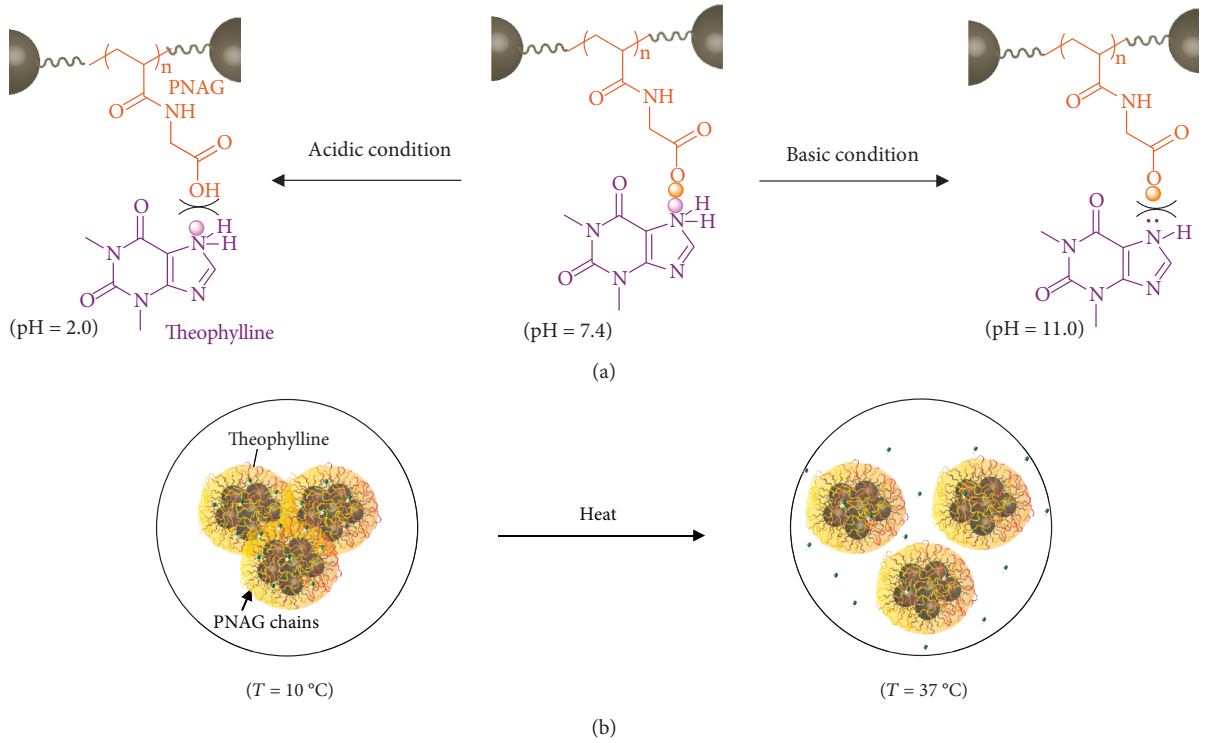

Figure 9: Proposed mechanisms of the theophylline release from the MNP nanocomposite triggered with (a) pH and (b) temperature changes.

At 37°C, the nanocomposite might be separated from each other due to the predominant interaction between PNAG on the nanocomposite surface and water molecules.

3.4. Drug Release Behavior. A showcase of the MNP nanocomposite for a drug controlled release application was also carried out in this work. Theophylline, a methylxanthine drug used in therapy for respiratory diseases, was selected as a model drug because it can be quantified via UV-vis spectrophotometry and possesses the amino groups in the structure. The protonation/deprotonation of the amino groups in theophylline leads to ionic adsorption/repulsion interactions with the carboxyl groups of PNAG, resulting in the drug release triggered by the change of the dispersion pH.

EE and DLE of the MNP nanocomposite crosslinked with 10 mol% of *tris*(2-aminoethyl)amine were first investigated. EE and DLE of the nanocomposite were 22–35% and 45–69%, respectively, depending on the pH and temperature of the dispersions. The effect of pH and temperature changes on the theophylline release rate from the MNP nanocomposite was then studied. The theophylline release studies were performed using stepwise pH changes from pH 7.4 to pH 2.0 and from pH 7.4 to pH 11.0 (Figures 8(a) and 8(b)). It should be noted that pK_a of PNAG was about 3.2 [38] and that of theophylline was 8.8 [39, 40]. It was found that the drug was rapidly released when the pH changed from neutral to acidic/basic conditions. This was attributed to the negatively charged repulsion of the deprotonated forms of PNAG (-COO^-) on the particle surface and theophylline in the basic condition (Figure 9(a)). Similarly, the positively charged repulsion of the protonated forms of these two components (-COOH of PNAG and $\equiv NH^+$ of theophylline) was rationalized for the abrupt release of the drug in the case of acidic condition.

The effect of the temperature change on the theophylline release behavior was also studied using a stepwise temperature change from 10°C to 37°C (Figure 8(c)). There was about 12% of the drug released at 10°C, and it was rapidly released for 92% when heated to 37°C. The abrupt release of the drug from the nanocomposite was attributed to the separation of the agglomerated nanocomposites at high temperature as indicated by the decrease in D_h (Figure 9(b)).

4. Conclusions

This work presented the preparation of pH- and thermoresponsive nanocomposite based on PNAG matrix and MNP and its application in drug controlled release. The MNP nanocomposite having good magnetic separation ability and water stability was obtained by tuning the types and concentrations of the crosslinkers. It exhibited dual-responsive properties as indicated by the change in its zeta potential and D_h when the environmental pH and temperature were changed. In addition, this novel nanocomposite was also demonstrated for use as a magnetically guidable vehicle for theophylline controlled release with pH- and thermotriggered mechanisms.

Data Availability

The data in the synthesis of PNAG-based magnetic nanocomposite and its drug release behavior used to support the findings of this study are included within the article and in the supplementary information file. All the raw data such as hydrodynamic size (D_h), zeta potential values, and drug release data used to support the findings of this study are available from the corresponding author upon request.

Conflicts of Interest

The authors declare that they have no conflicts of interest.

Acknowledgments

The authors thank the National Research Council of Thailand (NRCT) (R2562B093) for the support. MR especially acknowledges the Thailand Research Fund (TRF) (RSA5980002) for the financial funding. ND thanks the Science Achievement Scholarship of Thailand (SAST) for the scholarship.

Supplementary Materials

The supplementary file contains a ^1H NMR spectrum of NAG monomer, the calculations of the grafting density of carboxyl groups on PNAG-coated MNP after dispersing in water, and the calibration curves of theophylline in various conditions. *(Supplementary Materials)*

References

[1] A. Muñoz-Bonilla, J. Sánchez-Marcos, and P. Herrasti, "Conducting polymer hybrids," in *Springer Series on Polymer and Composite Materials*, V. Kumar, S. Kalia, and H. C. Swart, Eds., pp. 45–80, Springer International Publishing AG, Switzerland, 2017.

[2] J. Estelrich, E. Escribano, J. Queralt, and M. A. Busquets, "Iron oxide nanoparticles for magnetically-guided and magnetically-responsive drug delivery," *International Journal of Molecular Sciences*, vol. 16, no. 12, pp. 8070–8101, 2015.

[3] M. A. Willard, L. K. Kurihara, E. E. Carpenter, S. Calvin, and V. G. Harris, "Chemically prepared magnetic nanoparticles," *International Materials Review*, vol. 49, no. 3-4, pp. 125–170, 2013.

[4] B. Thong-On and M. Rutnakornpituk, "Controlled magnetite nanoclustering in the presence of glycidyl-functionalized thermo-responsive poly(*N*-isopropylacrylamide)," *European Polymer Journal*, vol. 85, pp. 519–531, 2016.

[5] S. Bucak, B. Yavuztürk, and A. D. Sezer, "Magnetic nanoparticles: synthesis, surface modifications and application in drug delivery," in *Recent Advances in Novel Drug Carrier Systems*, A. D. Sezer, Ed., pp. 165–200, IntechOpen, 2012.

[6] K. Petcharoen and A. Sirivat, "Synthesis and characterization of magnetite nanoparticles *via* the chemical co-precipitation method," *Materials Science & Engineering, B: Advanced Functional Solid-State Materials*, vol. 177, no. 5, pp. 421–427, 2012.

[7] M. Hetti, Q. Wei, R. Pohl et al., "Magnetite core-shell nanoparticles in nondestructive flaw detection of polymeric materials,"

ACS Applied Materials & Interfaces, vol. 8, no. 41, pp. 28208–28215, 2016.

[8] L. Xiao, J. Li, D. F. Brougham et al., "Water-soluble superparamagnetic magnetite nanoparticles with biocompatible coating for enhanced magnetic resonance imaging," *ACS Nano*, vol. 5, no. 8, pp. 6315–6324, 2011.

[9] N. N. Reddy, Y. M. Mohan, K. Varaprasad, S. Ravindra, P. A. Joy, and K. M. Raju, "Magnetic and electric responsive hydrogel-magnetic nanocomposites for drug-delivery application," *Journal of Applied Polymer Science*, vol. 122, no. 2, pp. 1364–1375, 2011.

[10] S. Panja, B. Saha, S. K. Ghosh, and S. Chattopadhyay, "Synthesis of novel four armed PE-PCL grafted superparamagnetic and biocompatible nanoparticles," *Langmuir*, vol. 29, no. 40, pp. 12530–12540, 2013.

[11] A. Pourjavadi, A. Abedin-Moghanaki, and S. A. Nasseri, "A new functionalized magnetic nanocomposite of poly(methylacrylate) for the efficient removal of anionic dyes from aqueous media," *RSC Advances*, vol. 6, no. 10, pp. 7982–7989, 2016.

[12] J.-M. Ringeard, P. Griesmar, E. Caplain et al., "Design of poly(*N*-acryloylglycine) materials for incorporation of microorganisms," *Journal of Applied Polymer Science*, vol. 130, no. 2, pp. 835–841, 2013.

[13] S. F. Medeiros, A. M. Santos, H. Fessi, and A. Elaissari, "Stimuli-responsive magnetic particles for biomedical applications," *International Journal of Pharmaceutics*, vol. 403, no. 1-2, pp. 139–161, 2011.

[14] J. Ge, Y. Hu, M. Biasini, W. P. Beyermann, and Y. Yin, "Superparamagnetic magnetite colloidal nanocrystal clusters," *Angewandte Chemie (International Ed. in English)*, vol. 46, no. 23, pp. 4342–4345, 2007.

[15] B. Luo, S. Xu, A. Luo et al., "Mesoporous biocompatible and acid-degradable magnetic colloidal nanocrystal clusters with sustainable stability and high hydrophobic drug loading capacity," *ACS Nano*, vol. 5, no. 2, pp. 1428–1435, 2011.

[16] S. Meerod, B. Rutnakornpituk, U. Wichai, and M. Rutnakornpituk, "Hydrophilic magnetic nanoclusters with thermo-responsive properties and their drug controlled release," *Journal of Magnetism and Magnetic Materials*, vol. 392, pp. 83–90, 2015.

[17] S. Khadsai, B. Rutnakornpituk, T. Vilaivan, M. Nakkuntod, and M. Rutnakornpituk, "Anionic magnetite nanoparticle conjugated with pyrrolidinyl peptide nucleic acid for DNA base discrimination," *Journal of Nanoparticle Research*, vol. 18, no. 9, 2016.

[18] C. Oka, K. Ushimaru, N. Horiishi, T. Tsuge, and Y. Kitamoto, "Core-shell composite particles composed of biodegradable polymer particles and magnetic iron oxide nanoparticles for targeted drug delivery," *Journal of Magnetism and Magnetic Materials*, vol. 381, pp. 278–284, 2015.

[19] S. Merino, C. Martín, K. Kostarelos, M. Prato, and E. Vázquez, "Nanocomposite hydrogels: 3D polymer-nanoparticle synergies for on-demand drug delivery," *ACS Nano*, vol. 9, no. 5, pp. 4686–4697, 2015.

[20] S. Davaran, S. Alimirzalu, K. Nejati-Koshki et al., "Physicochemical characteristics of Fe_3O_4 magnetic nanocomposites based on poly(*N*-isopropylacrylamide) for anti-cancer drug delivery," *Asian Pacific Journal of Cancer Prevention*, vol. 15, no. 1, pp. 49–54, 2014.

[21] S. Dutta, S. Parida, C. Maiti, R. Banerjee, M. Mandal, and D. Dhara, "Polymer grafted magnetic nanoparticles for delivery of anticancer drug at lower pH and elevated temperature," *Journal of Colloid and Interface Science*, vol. 467, pp. 70–80, 2016.

[22] Y. Prai-In, C. Boonthip, B. Rutnakornpituk et al., "Recyclable magnetic nanocluster crosslinked with poly(ethylene oxide)-*block*-poly(2-vinyl-4,4-dimethylazlactone) copolymer for adsorption with antibody," *Materials Science & Engineering. C, Materials for Biological Applications*, vol. 67, pp. 285–293, 2016.

[23] F. Li, J. Sun, H. Zhu, X. Wen, C. Lin, and D. Shi, "Preparation and characterization novel polymer-coated magnetic nanoparticles as carriers for doxorubicin," *Colloids and Surfaces. B, Biointerfaces*, vol. 88, no. 1, pp. 58–62, 2011.

[24] B. Koppolu, M. Rahimi, S. Nattama, A. Wadajkar, and K. T. Nguyen, "Development of multiple-layer polymeric particles for targeted and controlled drug delivery," *Nanomedicine*, vol. 6, no. 2, pp. 355–361, 2010.

[25] P. Theamdee, R. Traiphol, B. Rutnakornpituk, U. Wichai, and M. Rutnakornpituk, "Surface modification of magnetite nanoparticle with azobenzene-containing water dispersible polymer," *Journal of Nanoparticle Research*, vol. 13, no. 10, pp. 4463–4477, 2011.

[26] K. Kurd, A. A. Khandagi, S. Davaran, and A. Akbarzadeh, "Cisplatin release from dual-responsive magnetic nanocomposites," *Artificial Cells, Nanomedicine, and Biotechnology*, vol. 44, no. 3, pp. 1031–1039, 2016.

[27] N. Rodkate and M. Rutnakornpituk, "Multi-responsive magnetic microsphere of poly(*N*-isopropylacrylamide)/carboxymethylchitosan hydrogel for drug controlled release," *Carbohydrate Polymers*, vol. 151, pp. 251–259, 2016.

[28] I. M. El-Sherbiny, R. J. Lins, E. M. Abdel-Bary, and D. R. K. Harding, "Preparation, characterization, swelling and *in vitro* drug release behaviour of poly(*N*-acryloylglycine-chitosan) interpolymeric pH and thermally-responsive hydrogels," *European Polymer Journal*, vol. 41, no. 11, pp. 2584–2591, 2005.

[29] K. Deng, Q. Li, L. Bai et al., "A pH/thermo-responsive injectable hydrogel system based on poly(*N*-acryloylglycine) as a drug carrier," *Iranian Polymer Journal*, vol. 20, pp. 185–194, 2011.

[30] Z. M. O. Rzaev, S. Dinçer, and E. Pişkin, "Functional copolymers of *N*-isopropylacrylamide for bioengineering applications," *Progress in Polymer Science*, vol. 32, no. 5, pp. 534–595, 2007.

[31] W. Sun, Z. An, and P. Wu, "UCST or LCST? Composition-dependent thermoresponsive behavior of poly(*N*-acryloylglycinamide-*co*-diacetone acrylamide)," *Macromolecules*, vol. 50, no. 5, pp. 2175–2182, 2017.

[32] J. Seuring and S. Agarwal, "Polymers with upper critical solution temperature in aqueous solution," *Macromolecular Rapid Communications*, vol. 33, no. 22, pp. 1898–1920, 2012.

[33] J. Seuring, F. M. Bayer, K. Huber, and S. Agarwal, "Upper critical solution temperature of poly(*N*-acryloyl glycinamide) in water: a concealed property," *Macromolecules*, vol. 45, no. 1, pp. 374–384, 2012.

[34] B. A. Pineda-Contreras, H. Schmalz, and S. Agarwal, "pH dependent thermoresponsive behavior of acrylamide-acrylonitrile UCST-type copolymers in aqueous media," *Polymer Chemistry*, vol. 7, no. 10, pp. 1979–1986, 2016.

[35] A. Gandhi, A. Paul, S. O. Sen, and K. K. Sen, "Studies on thermoresponsive polymers: phase behaviour, drug delivery and biomedical applications," *Asian Journal of Pharmaceutical Sciences*, vol. 10, no. 2, pp. 99–107, 2015.

[36] M. A. Ward and T. K. Georgiou, "Thermoresponsive polymers for biomedical applications," *Polymer*, vol. 3, no. 3, pp. 1215–1242, 2011.

[37] Y. Zhang, S. Chen, M. Pang, and W. Zhang, "Synthesis and micellization of a multi-stimuli responsive block copolymer based on spiropyran," *Polymer Chemistry*, vol. 7, no. 45, pp. 6880–6884, 2016.

[38] K. L. Deng, H. B. Zhong, T. Tian, Y. Gou, Q. Li, and L. R. Dong, "Drug release behavior of a pH/temperature sensitive calcium alginate/poly(*N*-acryloylglycine) bead with core-shelled structure," *Express Polymer Letters*, vol. 4, no. 12, pp. 773–780, 2010.

[39] A. A. Elouzi, F. Abeid, M. Almegrhe, and M. El-Baseir, "Acidic beverage and the bioavailability of theophylline," *Journal of Chemical and Pharmaceutical Research*, vol. 4, pp. 3454–3459, 2012.

[40] M. Shalaeva, J. Kenseth, F. Lombardo, and A. Bastin, "Measurement of dissociation constants (pK_a values) of organic compounds by multiplexed capillary electrophoresis using aqueous and cosolvent buffers," *Journal of Pharmaceutical Sciences*, vol. 97, no. 7, pp. 2581–2606, 2008.